TRANSITION RADIATION FROM A CYLINDRICAL TARGET AND TRANSVERSE BEAM SIZE DIAGNOSTICS*

A.P. Potylitsyn†, Tomsk Polytechnic University, Tomsk, Russia
L.G. Sukhikh, DESY, Hamburg, Germany

Abstract

In this paper we propose to use backward transition radiation from a cylindrical target in EUV region in order to determine transverse beam size without any additional optics.

INTRODUCTION

Transverse profile diagnostics in modern electron linear accelerators is mainly based on backward transition radiation (BTR) in optical region. Advantages of optical BTR are a linear response and the rather high light output emitted in a small cone with an opening angle defined by the beam energy. However, for modern FELs like Linac Coherent Light Source LCLS in Stanford (USA) [1] and FLASH at DESY in Hamburg (Germany) [2] the use of optical radiation fails because of coherence effects in the emission process.

The optical BTR diagnostics also fails because of the diffraction limit for sub-micron and nano-beams that are the goal for future electron-positron collider. It was shown at KEK-ATF2 in Tsukuba (Japan) by A.Aryshev et al. [3], where authors had so small beam size that it was possible to measure a Point Spread Function (PSF) of standard imaging technique based on optical BTR.

Earlier it was proposed to use BTR in EUV region in order to reduce diffraction limit and suppress coherent radiation [4] and an experiment devoted to the investigation of the characteristics of EUV BTR from a flat target was carried out [5, 6]. In order to obtain bunch profile in the scheme with flat target one needs focusing multilayer mirror that should be situated in vacuum. This makes the adjustment of the optics a nontrivial task. In this paper we propose to use BTR radiation in EUV region generated by a cylindrical target. In this case one may avoid the use of focusing mirror.

Let us assume that we have some Gaussian beam of real photons with rms σ that reflects from a cylindrical surface as it is shown in Fig. 1. In this case on the detector surface one obtains a magnified image of the initial beam (neglecting the aberrations) with rms $\sigma_d \simeq \sigma \left(1 + \frac{2L}{R \cos \psi_0}\right)$, where L is the distance to the detector, R is the cylinder radius, ψ_0 is the incidence angle. The electromagnetic field

of an ultra-relativistic electron is close to the field of the plane wave and may be treated as virtual photons. The main difference between real and virtual photon reflection is PSF. In the case of single electron the spatial distribution of emitted radiation on the detector have well-known structure with minimum along specular reflection direction. For the flat target the maximum of distribution is situated under the angle $\theta = \gamma^{-1}$, where γ is the electron Lorentz-factor. The spatial distribution from the cylindrical target is defocused, i.e. the maximum is situated under the angle $\theta > \gamma^{-1}$. The convolution of the PSF with transverse beam profile gives the image on the detector. Depending on the beam energy, cylinder radius, radiation wavelength and observation geometry one may obtain the distribution on the detector that gives either beam size estimation or beam profile information.

THEORETICAL MODEL

Theoretical calculations are based on a generalized surface current method [7]. The calculation scheme is shown in Fig. 1. The radiation field on the detector plane $\mathbf{E_d}(\mathbf{r}, \omega)$ for the central electron may written as following:

$$\mathbf{E_d}(\mathbf{r}, \omega) = \frac{1}{2\pi} \int_S dS' \left[[\mathbf{n}(\mathbf{r}'), \mathbf{E_e}(\mathbf{r}', \omega)], \nabla G(\mathbf{r}', \mathbf{r}, \omega)\right], \quad (1)$$

where $\mathbf{n}(\mathbf{r}')$ is the surface normal vector, $\mathbf{E_e}(\mathbf{r}', \omega)$ is the electron field, $\nabla G(\mathbf{r}', \mathbf{r}, \omega)$ is the Green function gradient,

Figure 1: Simulation scheme and some definitions. We assume that $\sigma \ll R$

Figure 2: The angular distributions of the BTR from different targets: black curve – flat target, blue curve – cylindrical target $R = 50$ mm, red curve – cylindrical target $R = 25$ mm, green curve – cylindrical target $R = 10$ mm.

dS' is the surface element. The integration is performed over the cylindrical surface S. The normal vector may be written as:

$$\mathbf{n}(\mathbf{r}') = \left\{ 0, \frac{y' - R\sin\psi_0}{R}, -\frac{\sqrt{R^2 - (y' - R\sin\psi_0)^2}}{R} \right\}, \tag{2}$$

where R is the cylinder radius. The field of the electron traveling along z axis may be written as:

$$\mathbf{E_e}(\mathbf{r}', \omega) = \frac{2e\omega}{\beta^2\gamma 2\pi c^2} \exp\left[i\frac{\omega}{\beta c}z'\right] \times$$
$$\left\{ \begin{array}{l} \frac{x'}{\sqrt{x'^2 + y'^2}} K_1\left(\frac{\omega}{\beta c\gamma}\sqrt{x'^2 + y'^2}\right) \\ \frac{y'}{\sqrt{x'^2 + y'^2}} K_1\left(\frac{\omega}{\beta c\gamma}\sqrt{x'^2 + y'^2}\right) \\ -\frac{i}{\gamma} K_0\left(\frac{\omega}{\beta c\gamma}\sqrt{x'^2 + y'^2}\right) \end{array} \right\} \tag{3}$$

Here e is the electron charge, β is the electron velocity in the speed of light units, c is the speed of light, γ is the electron Lorentz-factor, K_0, K_1 are the modified Bessel functions of the second kind (McDonald functions) of the zero and first order, respectively. For the cylindrical target $z' = R\cos\psi_0 - \sqrt{R^2 - (y' - R\sin\psi_0)^2}$.

The gradient of Green function may be written as:

$$\nabla G(\mathbf{r}', \mathbf{r}, \omega) = \frac{\mathbf{r}' - \mathbf{r}}{|\mathbf{r}' - \mathbf{r}|^2} e^{i\frac{\omega}{c}|\mathbf{r}' - \mathbf{r}|} \left(i\frac{\omega}{c} - \frac{1}{|\mathbf{r}' - \mathbf{r}|}\right) \tag{4}$$

The observation point vector $\mathbf{r}$ may be written as:

$$\mathbf{r} = A(2\psi_0). \{\theta_x L, \theta_y L, -L\}, \tag{5}$$

where $A(2\psi_0)$ is the ordinary rotation matrix.

The element of surface dS' may be written as:

$$dS' = dx'dy' \frac{1}{\sqrt{R^2 - (y' - R\sin\psi_0)^2}} \tag{6}$$

Substituting Eqs. (2)–(6) to Eq. (1) one may obtain the radiation field of BTR, generated by the single electron. The radiation spectral-angular density may be written as:

$$\frac{d^2 W}{\hbar d\omega d\Omega} = \frac{cr^2}{\hbar} |\mathbf{E_d}(\mathbf{r}, \omega)|^2, \tag{7}$$

where $\hbar$ is the Plank constant.

As it was mentioned before, the BTR generated by the cylindrical target is defocused, i.e. the distance between radiation maxima is more than $2\gamma^{-1}$ in spite of the detector situated in far-field (wave) zone. Figure 2 shows an example of angular distribution of BTR from the cylindrical target. The calculation was carried out using Eq. (7) for the following parameters: $\gamma = 2500$, $\psi_0 = 67.5°$, $\lambda = 15$ nm, $\theta_x = 0$, $L = 5000$ mm. The angle $\psi_0 = 67.5°$ was chosen because of the high reflectivity of some materials in EUV region at small grazing angles of incidence. In transverse direction (along θ_x) the angular distributions from the different cylinders have the distance between radiation maxima equal to $2\gamma^{-1}$ (see Fig. 2).

Let us assume that we have some electron beam with normalized transverse distribution $\rho(x, y)$ that radiates incoherently. In this case the spectral-angular distribution of BTR may be written as:

$$\frac{d^2 W_b}{\hbar d\omega d\Omega} =$$
$$\frac{cr^2}{\hbar} \int dx'' dy'' |\mathbf{E_d}(x - x'', y - y'', z, \omega)|^2 \rho(x'', y'') \tag{8}$$

In order to simplify the calculations we assume that $\rho(x, y) = \rho(y)\delta(x)$, where $\delta(x)$ is the Dirac delta function.

Figure 3 shows an example of the calculated BTR distributions for different bunch vertical sizes. In this calculation we assume that we have Gaussian beam $\rho(y) = \frac{1}{\sqrt{2\pi}\sigma} \exp\left[-\frac{y^2}{2\sigma^2}\right]$. From Fig. 3 one may see that the single electron distribution is significantly changed by the transverse beam size effect. Depending on the beam size there are two ways to estimate it. In a case of small beam
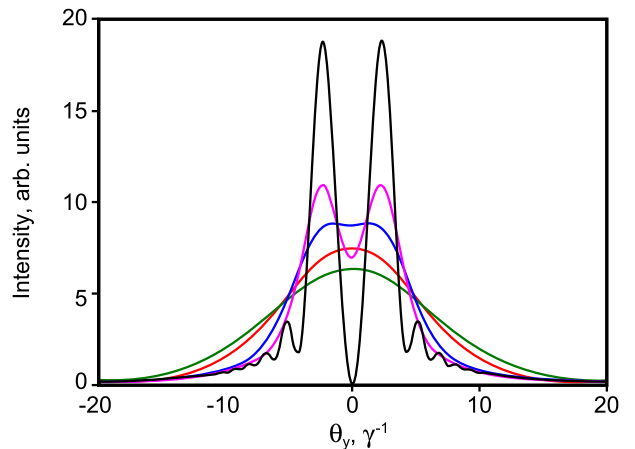

Figure 3: Angular distributions of BTR for different vertical bunch sizes. $\gamma = 2500$, $\lambda = 15$ nm, $R = 50$ mm, $\psi_0 = 67.5°$. Black curve – single electron distribution, pink – $\sigma = 5\,\mu$m, blue – $\sigma = 8\,\mu$m, red – $\sigma = 15\,\mu$m, green – $\sigma = 20\,\mu$m.
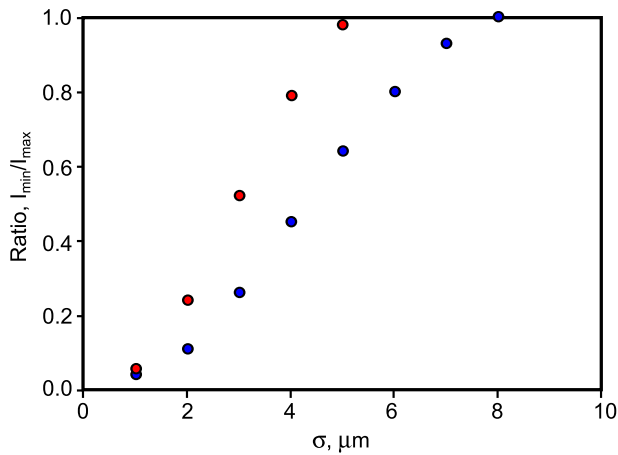
Figure 4: Calibration curve for small Gaussian beams. $\gamma = 2500$, $\lambda = 15\,\text{nm}$, $\psi_0 = 67.5°$. Blue dots – $R = 50\,\text{mm}$, red dots – $R = 25\,\text{mm}$.

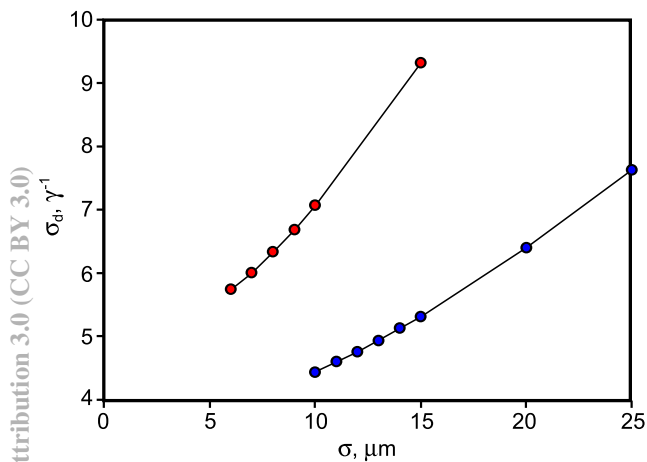
Figure 5: Calibration curve for large Gaussian beams. $\gamma = 2500$, $\lambda = 15\,\text{nm}$, $\psi_0 = 67.5°$. Blue dots – $R = 50\,\text{mm}$, red dots – $R = 25\,\text{mm}$.

sizes (pink curve in Fig. 3) one may calculate a ratio of central gap intensity to intensity in distribution maximum. This ratio depends on the beam size and is equal to zero for a single particle. In a second case (red and green curves in Fig. 3) one may estimate the beam size using some characteristic size of obtained distribution, e.g. a distribution rms for Gaussian beam shown in Fig. 3.

Figure 4 shows the calibration curve (ratio of the central gap intensity to the intensity in distribution maximum versus the vertical beam size) for small beams for two different cylinder radii.

Figure 5 shows the calibration curve for large beams (dependence of the obtained distribution rms versus the vertical beam size) for two different cylinder radii.

In Figs. 4 and 5 one may see that the spatial distribution of BTR in EUV region from the cylindrical target is very
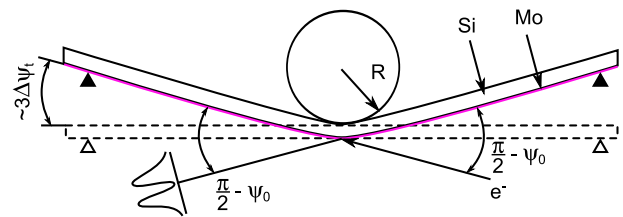
Figure 6: The scheme of bent silicon crystal covered with molybdenum that can be used as cylindrical target.

sensitive to small changes of the beam size. For large beam size measurements one may use larger cylinders.

CONCLUSION

As conclusion it is important to mention that one may use BTR from cylindrical target in order to obtain beam transverse size and profile without any additional focusing optics. According to our calculations the proposed technique is very sensitive to even micron changes of the beam size (using cylinder with $R = 25\,\text{mm}$). Using smaller cylinders one may obtain even better resolution.

The single electron spatial distribution from the cylindrical target is wider than ordinary PSF from the flat target. However, the cylinder target imaging may be useful in some applications where the use of external optics is inconvenient.

From the practical point of view one may use bent silicon crystal covered by some metal that have good reflectivity in EUV region, e.g. molybdenum. Figure 6 shows the possible bent target following Ref. [8].

REFERENCES

[1] H. Loos et al., Proc. FEL '08, Gyeongju (South Korea), 485-489 (2008).

[2] S. Wesch, C. Behrens, B. Schmidt, P. Schmüser, Proc. FEL '09, Liverpool (UK), 619-622 (2009).

[3] Aryshev, A., Terunuma, N., Urakawa, J., Boogert, S.T., Karataev, P., Howell, D., Proc. IPAC '10, Kyoto, (Japan), 193-195 (2010).

[4] L.G. Sukhikh, S.Yu. Gogolev , and A.P. Potylitsyn , Nucl. Instrum. Methods Phys. Res., Sect. A **623**(1), 567-569 (2010)

[5] L.G. Sukhikh, D. Krambrich, G. Kube, W. Lauth, Yu.A. Popov, and A.P. Potylitsyn, SPIE Optics and Optoelectronics proceedings, 18-21 April, Prague (2011), to be published.

[6] L.G. Sukhikh, D. Krambrich, G. Kube, W. Lauth, Yu.A. Popov, and A.P. Potylitsyn, Proc. DIPAC '11, Hamburg, (Germany), WEOA02 (2011).

[7] D.V. Karlovets and A.P. Potylitsyn, "Generalized surface current method in macroscopic theory of diffraction radiation", Phys. Lett. A **373**, 1988-1996 (2009).

[8] V.M. Biryukov, Yu.A. Chesnokov, and V.I. Kotov, "Crystal Channeling and Its Application at High-Energy Accelerators", Springer Berlin (1997).